



# 3D FE analysis of urban asphalt pavements on public transport roads under a rolling bus tyre

Análise em EF 3D de pavimentos asfálticos urbanos em vias de transporte público sob ação de pneu de ônibus em movimento

# Neusa Eliana Figur<sup>1</sup>, Daniane Franciesca Vicentini<sup>1</sup>

<sup>1</sup>Universidade Federal do Paraná, Curitiba, Paraná, Brasil

Contact: neusafigur@hotmail.com, ((NEF); vicentini@ufpr.br, ((DFV))

#### Submitted:

27 March, 2025

#### Revised:

19 July, 2025

## Accepted for publication:

1 August, 2025

## **Published:**

27 November, 2025

#### **Associate Editor:**

Francisco Thiago Sacramento Aragão, Universidade Federal do Rio de Janeiro, Brasil

#### **Keywords:**

Dynamic analyses.
Flexible pavements.
Acceleration and braking.
Longitudinal grade.
Finite elements.

## Palavras-chave:

Análises dinâmicas. Pavimentos flexíveis. Aceleração e frenagem. Declividade longitudinal. Elementos finitos.

DOI: 10.58922/transportes.v33.e3111



#### **ABSTRACT**

Understanding the structural mechanisms at which the asphaltic pavements are subjected in the field can prevent premature failure. In this work, dynamic and static 3D finite element analyses were performed and compared among themselves to evaluate their effects in terms of constant speed, acceleration, braking, roughness and longitudinal slopes of the roadway. Numerical analysis is a non-destructive research method which allows access to the response at any internal point of the pavement in a more economic and sustainable way. A common urban pavement section was chosen for the analyses as being representative of passenger transportation routes in Curitiba – Brazil. A standard bus was considered for the analyses and the parameters simulated diverse and usual traffic and service conditions. According to this analysis, acceleration in downward slopes represents the most critical situation for the pavement under study, reaching values up to 24 times greater than those in the static condition.

## RESUMO

Entender os mecanismos estruturais aos quais os pavimentos asfálticos estão submetidos em campo pode prevenir falhas prematuras. Neste trabalho, análises dinâmicas e estáticas de elementos finitos 3D foram realizadas e comparadas entre si para avaliar seus efeitos em termos de velocidade constante, aceleração, frenagem, rugosidade e declives longitudinais da rodovia. A análise numérica é um método de pesquisa não destrutivo que permite acessar a resposta em qualquer ponto interno do pavimento, de forma mais econômica e sustentável. Um trecho comum de pavimento urbano foi escolhido para as análises por ser representativo de rotas de transporte de passageiros em Curitiba — Brasil. Um ônibus padrão foi considerado para as análises e os parâmetros simularam condições diversas e usuais de tráfego e serviço. De acordo com esta análise, a aceleração em declives é a situação mais crítica para o pavimento em estudo, podendo ser até 24 vezes maior que a condição estática.

## 1. INTRODUCTION

Much has been discussed about the durability of flexible pavements in face of various traffic demands, especially in corridors where, due to the peculiarities and circumstances of traffic, drivers have to constantly change vehicle speeds, adjusting them according to the flow.

Such circumstances can cause significant horizontal stresses in pavements, enhanced by distresses that appear in regions near speed humps, traffic lights, intersections, curves, ramps, bus stops or tolls. These in turn, together with vertical loading (Farias, 1997), can reach significant tensile stresses near the pavement surface.

It is sometimes possible to identify, in asphaltic pavements, transverse ripples along the longitudinal axis of the road (Figure 1a). This type of defect, of the order of few centimetres, is due to asphalt mass flow (DNIT, 2013) and it is related to the horizontal shear stress generated by vehicles in areas subjected to vehicle acceleration/deceleration (CNT, 2018).





**Figure 1.** (a) Corrugations at the intersection between 24 de Maio Street with the bus rapid transit (BRT) corridor at Sete de Setembro Avenue, in Curitiba (on May, 2018); (b) Standard 2CB type of public transportation vehicle under study.

Despite significant, dynamic effects are neglected in most current design procedures and in flexible pavements evaluations, where usually only static vertical loads are considered on the pavement surface, which can result in a significant impact on the mechanical performance of the pavement (Khavassefat, Jelagin and Birgisson, 2014).

The asphalt pavement, if compared with other engineering structures, has a reduced service life, usually from 10 to 20 years. Thus, it is important to value more complete design strategies, which could consider all the active stresses and intervening factors. And certainly, this could contribute

to the optimization of the pavement structure, increasing its durability, as well as reducing the costs with restoration and maintenance (Medina and Motta, 2015).

These benefits could also be applied to urban roads, the object of this study, especially in bus corridors. The city of Curitiba, for example, has been considered as a reference to the public transportation system and has inspired several cities in Brazil and the world (Seco, 2016). Previously to the COVID-19 pandemic period, the Integrated Transport Network (ITN) had 83 km of corridors, highways or exclusive bus lanes for BRT, outlining the so-called transport corridor, with a total of 1,280 buses in an operational fleet and 303,769 km travelled on average per working day (URBS, 2017a; 2017b).

But the need for exclusive bus lanes and the channelization of traffic into 'corridors' require special attention regarding the effects of the additional loads resulting from vehicle acceleration and braking, especially at bus stops, where permanent deformation of the asphalt layer is expected (Medina and Motta, 2015).

Searching for critical efforts (mainly in terms of displacements, longitudinal and shear stresses) with potential for failure initiation, especially in bus corridors, the aim of this work is to simulate (by building a 3D Finite Element model) the dynamic effects of a standard vehicle (Figure 1b) on a common flexible pavement due to vertical and horizontal loads under acceleration, braking and constant speed for determined service conditions (roughness and longitudinal grade of the roads), analysed against themselves.

## 2. PARAMETERS UNDER ANALYSIS

Around the 1970s, with the development of computer technology and the popularization of the Finite Element Method (FEM), more sophisticated studies about dynamics on the roadway structure became possible to conduct (Schmidt and Mazzilli, 2017). In the last decades, some researchers, such as Saleh, Mamlouk and Owusu-Antwi (2000), Hammoum et al. (2010) and Feng et al. (2012), have found some factors that could influence the behaviour and the stresses in pavements. Horizontal loads produced during vehicle motion and longitudinal grade are some examples of these factors, selected for study in this paper, and discussed in more detail below.

# 2.1. Speed variation

During the acceleration or braking process of a moving vehicle, a set of horizontal and vertical components of effort is produced. At braking, for example, a load transfer from rear axles to front axles commonly occurs. This shift in weight distribution leads to the generation of stresses at the interface between the tyres and the pavement. Then, especially in the last decade, some studies (Hammoum et al., 2010; Zhang and Wang, 2010; Hajj et al., 2012; Feng et al., 2012; Nonde, 2014) have addressed the effects of horizontal loads on stress distribution in pavements, among which, Hammoum et al.'s (2010) work can be highlighted. They studied the responses on bituminous pavement at various depths of its structure and under dynamic loading conditions, noticing a significant increase of the shear stresses at near-surface for both conditions: acceleration and braking.

The importance of considering horizontal loads was also observed in Zhang and Wang (2010) and Nonde (2014) studies. The first ones observed that the crack depth in hot-mix asphalt (HMA) is much higher in pavements subjected to braking conditions. They also noticed a decrease in the number of cycles for fatigue failure when compared to the no braking condition. Nonde (2014)

found that when vertical and horizontal load components are applied both together, significant horizontal displacement can be observed between the layers. The author explained that the horizontal stress induced by the vehicle braking and acceleration crushes the aggregates and densifies the HMA, reducing the air voids, promoting loss of stability and wrinkling the asphaltic concrete (AC) layer. This also produces loss of strength and sliding, because when the bonding between the AC and the base layer is weak, the stress transfer capacity between these layers decreases. When it cannot withstand the local horizontal stress induced by the vehicle braking, sliding cracking occurs, starting at the surface towards the bottom of the AC layer.

Working with an implicit dynamic analysis, Assogba et al. (2021) created a full-scale 3D model in a FE semi-rigid pavement configuration. They verified that a decrease in vehicle speed led to an increase in the loading duration, which could affect fatigue performance.

# 2.2. Roadway slope

In addition to the issue of the horizontal force's effects, Yang et al. (2010) analysed the effects of different slopes on the maximum shear stress and vertical strain in the surface course of asphalt mixture. Their study also examined the influence of traffic load and vehicle speed on road sections with and without slopes. The findings revealed that the maximum shear stress and vertical strain increase with slope and traffic load, while decreasing with speed. The middle layer (located at 4 to 10 cm below the road surface) generally exhibited higher maximum shear stress and vertical strain than other layers. Therefore, improving the rutting resistance of the middle layer is crucial for effectively addressing rutting damages in long-steep longitudinal slopes.

Chen, Wang and Mu (2011) also studied longitudinal grades of roadways. They have found an increase in the maximum shear stress amplitude to more than double when the longitudinal slope increased from 0% to 7%. This could lead to the impaired pavement, as well as sliding and early fatigue failure, for example.

The occurrence of rutting in asphalt pavement is particularly more problematic in road sections with a longitudinal slope than those without any slope (Li and Li, 2012). The reason for this is that the slope reduces the average speed of vehicles traveling upslope, resulting in a significant increase in total loading time. When large longitudinal grades are present at the geometry of the road and the pavement receives vertical and horizontal stresses, more severe overloads are produced (Li and Xin, 2014).

Zhang, Yang and Ma (2020) explored potential solutions to mitigate wheel rutting, uplift, fatigue cracking, and other common issues observed in sharp curves or steep slopes. They conducted a comparative analysis of different mechanical models for asphalt pavement structures under such conditions and found that the use of a high modulus AC can significantly reduce longitudinal or transverse deformation and prevents fatigue cracking of the AC.

Considering geometric parameters, Yin et al. (2020) presented an interesting work aiming at roadway safety, where the influence of road geometry on rollover and skidding was studied for SUV vehicles at 80km/h. They studied combined parameters, such as pavement surface friction, motion on vertical and horizontal curves, super-elevation and longitudinal slope, identifying critical situations to avoid.

## 3. THE 3D FE DYNAMIC MODEL

The authors mentioned in previous section achieved some progress in studying the pavement under dynamic loads for different approaches, using more simplified models for their analysis (generally quasi static analysis, with the wheel as a concentrated moving load, despite this is not able to capture the induced effects of inertia on the pavement, as the damping and the frequence-dependent materials). Thus, in this study, a dynamic analysis was used to better simulate the tyre moving loads.

A rear wheel of a moving bus (from Figure 1b) was modelled in a 3D FE explicit dynamic symmetric model, over an urban pavement. The wheel is rolling over the surface, while this action instantaneously transfers efforts to the pavement through the contact. This study was applied to a common urban pavement section on public transport roads, detailed next.

# 3.1. Pavement and tyre materials

The pavement section and the tyre studied in this work are represented in Figure 2.

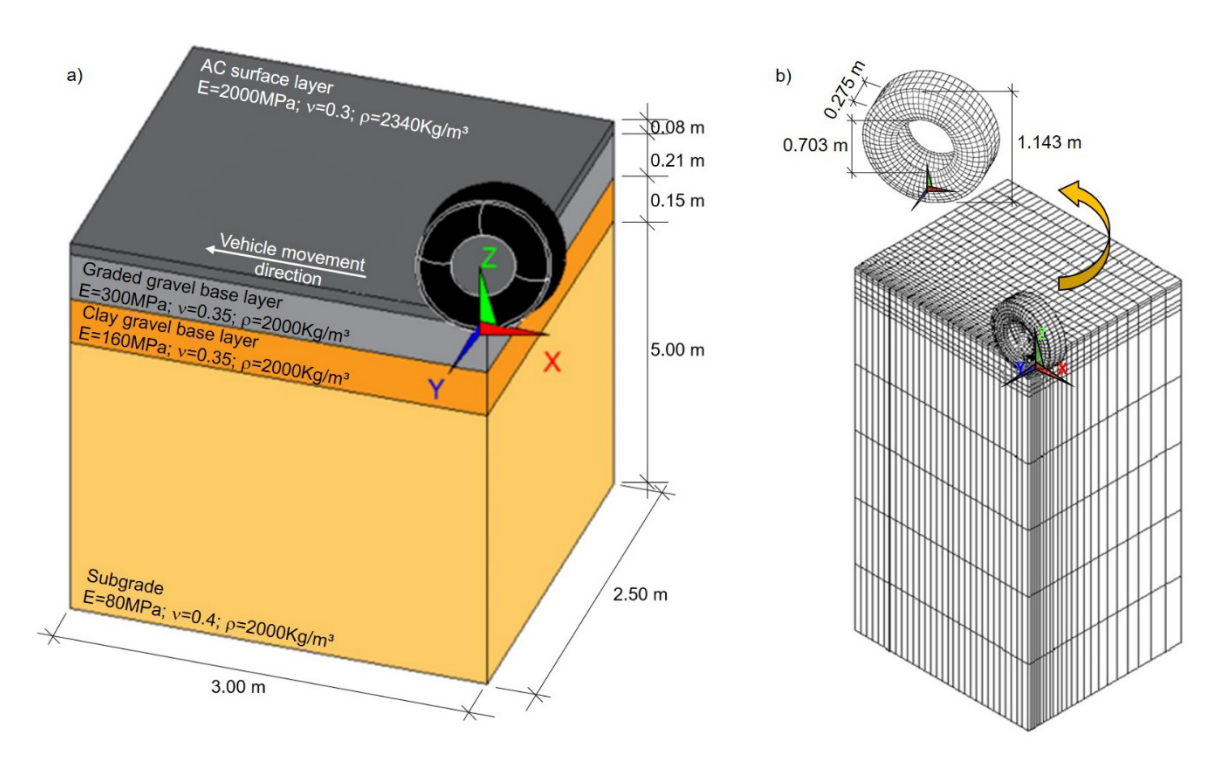


**Figure 2.** Flexible pavement section under study: (a) 3D geometry with the material properties; (b) FE tyre-pavement model showing the mesh and the tyre geometry detail.

From Figure 2a, E is the resilient modulus (in MPa, a constant parameter, so that it can be taken as the Young's modulus in this work),  $\rho$  is the density of the material (kg/m³) and v is the Poisson's ratio. For consistency with the assumption of infinite medium (since the FE model must be finite), the subgrade layer was taken as a 5.00 m deep soil. In this work, all pavement materials were considered in linear elastic behaviour and the analysis was carried out in an explicit dynamic type. Elasticity is usually conservative, which is an approximation from mechanics, and it is widely used in pavement analysis, either as a part of the hypothesis of some experimental or field testing

(i.e. AEMC software, back calculation procedures, pavement deflection testing, resilient modulus calculation from LVDT, etc.), so this simplification does not compromise the results of this work at all.

The pavement structure and their properties were obtained from laboratory and field studies carried out by the Research and Urban Planning Institute of Curitiba (IPPUC, in Portuguese) and the Federal University of Paraná through a collaboration Project (number 23075.042993/2013-41). Such studies covered the survey of the characteristics of asphaltic pavements which started to receive intense bus traffic along the years, and the section presented in Figure 2a was present throughout several regions in the city of Curitiba.

The applied load considered the tyre 275/80 R22.5 type, corresponding to a half of the rear tyre for the 2CB vehicle type, shown in Figure 1b, where 275 is the tyre width in millimetres, 80 means that the tyre height is equal to 80% of its width, and R22.5 is the code for the nominal rim radius (i.e., 22.5 inches or 571.5 mm).

The tyre properties required as input data for the model are the equivalent Young's modulus (E = 6894.8 MPa), v = 0.5 is the Poisson's ratio,  $g = 9.81 \text{ m/s}^2$  is the gravitational acceleration and p = 0.76 MPa is the tyre inflation (standard pressure for 2CB vehicle). Their characteristics have been selected in the software database for hyperelastic materials, being consistent with the literature (Ghoreishy, 2006; Meyers and Chawla, 2009; Giurgiu, Ciortan and Pupaza, 2013).

This type of bus collects passengers and covers regular routes, interconnecting the districts and the terminals along the city, performing an important role in the ITN of Curitiba.

# 3.2. 3D FE model and parameters

In dynamic analysis by direct integration over time, numerical integration procedures (implicit or explicit) can be applied. The implicit strategy generally is more used in pavement problems, because it presents less convergence problems. While this method computes the displacements at any time t by solving a set of non-linear equations at t-1 time, the explicit method adds the increment of displacements between t and t-1 in the displacements at t-1 time, calculated by double integration of the acceleration, from dynamic equations in that degree of freedom. This simplifies the implementation of models for more complicated materials, with changings in restrictions and loading conditions and because of this, the explicit strategy was chosen for this work.

The dynamic problem seeks to balance external actions with the internal ones:

$$M\ddot{u}(t) + C\dot{u}(t) + Ku(t) = F_{\text{ext}}(t) \tag{1}$$

where M, C and K are the mass, dumping and the stiffness matrixes, respectively. The vectors  $\ddot{u}$ ,  $\dot{u}$  and u are time dependent, being acceleration, speed and displacement, respectively. The  $F_{\rm ext}$  is the external forces vector (i.e., the applied loads, generally).

For an incremental explicit scheme, the Equation 1 can be rewritten considering a residual vector  $F_{\rm res}$ :

$$\ddot{u}^n = M^{-1}(F_{\text{ext}}^n - F_{\text{int}}^n + F_{\text{res}}^n)$$
 (2)

where n is the current step and  $F_{int}^n$  is the vector that gathers the internal forces resulting from the stiffness and damping components.

To the next time-step, time integration by central differences is used:

$$\dot{u}_{n+\frac{1}{2}} = \dot{u}_{n-\frac{1}{2}} + \Delta t_n \ddot{u}_n \tag{3}$$

$$u_{n+1} = u_n + \Delta t_{n+\frac{1}{2}} \dot{u}_{n+\frac{1}{2}} \tag{4}$$

where:

$$\Delta t_{n+\frac{1}{2}} = \frac{\Delta t_n + \Delta t_{n+1}}{2} \tag{5}$$

As the explicit solution method uses information only from the current state (t = n) to predict the displacement field in the subsequent state (t = n+1), half of the time increment  $(n + \frac{1}{2} \text{ and } n - \frac{1}{2})$  is used for the subsequent state and previous state before to (t = n), respectively.

The geometry is then updated by adding displacement increments to the initial geometry:

$$x_{n+1} = x_0 + u_{n+1} \tag{6}$$

where  $x_{n+1}$  is the nodal position at the subsequent instant,  $x_0$  is the initial position and  $x_{n+1}$  is the displacement given by the time increment n.

Therefore, time integration is explicit in the sense that, once the acceleration  $\ddot{u}_n$  is known at the current instant, the velocities and displacements for a later time (n+1) are calculated from values known only at the previous time (n).

In this work, a 3D FE model was developed from the geometry shown in Figure 2a. In such model, vertical displacement constraints at the bottom of the subgrade layer were considered, as well as horizontal constraints at the vertical faces, as recommended by Zaghloul and White (1993); Kuo, Hall and Darter (1995) and Saad, Mitri and Poorooshasb (2005).

In order to reduce computational efforts, symmetry planes were applied to the model and only one tyre was considered. The standard vehicle from Figure 1b has a single axle with dual wheel (SADW), with 100 kN maximum load at the rear axle (DNIT, 2012). In the model, the applied load ( $P=25~\rm kN$ ) corresponds to a quarter of the rear axle of this vehicle.

Considering that the model domain must be large enough to avoid edge influences, extra effort was made in order to obtain dimensions that could keep the size of the problem manageable in computing time, within the scope of the analysis of interest and considering the computer storage requirements. Following previous experience (Medina and Motta, 2015), a suitable lateral boundary should be at least twenty times larger than the radius of the loaded area, and a subgrade layer depth about fifty times that radius, in order to simulate an infinite medium.

The pavement structure was modelled in the ANSYS computer program, using the SOLID 164 element, a hexahedral FE with eight nodes and nine degrees of freedom at each node: displacements, velocities, and accelerations in the X, Y and Z directions (Figure 2).

The mesh of the tyre model was generated by using rectangular FE type SHELL163, a 4-node plane element with bending capacity (in modelling bodies such as curved surfaces, for example) and membrane, with 12 degrees of freedom at each node: translation, velocities and accelerations in the X, Y and Z nodal directions, and rotation around the same nodal axes (Figure 2b).

The tyre was considered as a hyperelastic behaviour material, and its equivalent density was determined by the ratio between the wheel load and the volume of the modelled region of the tyre (considered with 1mm thickness for the SHELL163 FE). Angular velocities were also needed into the dynamic model, and adjusted according to the speed under study.

When using FEM, it is necessary to balance mesh refinement (in order to obtain adequate results) with computational costs. The model mesh presented here was tested several times (Figur, 2019) until the response converged (i.e., the refinement above which the results no longer changed). Figure 2b shows the final mesh, with 9900 FE in total. This mesh was used in both: the static and dynamic models for comparison purposes.

For this work, the automatic surface-to-surface contact (ASTS, available in the software library) was adopted to simulate the tyre-pavement interaction. The model used in these analyses considered the full adherence between layers, not allowing the relative sliding between them (thus reactions arise in order to counterbalance this effect). In the field, however, slipping between layers may occur when interlayer treatments are neglected (as for example, the absence of a tack coat, as well as the incorrect cleaning of the previous layer before applying the bonding product).

In order to analyse the pavement behaviour when subjected to dynamic loads, different parameters were selected for this work.

Considering speed cases, in this study the acceleration a=0 was simulated by keeping constant speed during the entire tyre movement, along the X axis. For variable speeds (i.e.,  $a \ne 0$ , the wheel started from the resting condition (0 km/h) until to reach some usual established speed limits, i.e., 20, 40 and 60 km/h from Brazilian Traffic Standard Code (Brasil, 1997), in order to simulate accelerating conditions (a > 0). The braking condition was simulated in an analogous manner, but starting from the established speed to 0 km/h (decelerating, i.e., a < 0).

The coefficient of dynamic friction (FS) was computed from the definition of three adherence situations, given by the International Friction Index (IFI) for pavements (DNIT, 2006; Figur, 2019; ASTM, 2023). FS is a dimensionless parameter, speed dependent, and it was calculated aiming to represent three surface conditions: smooth, intermediate, and rough condition (in the model, FS = 0.60; 0.68 and 0.87, respectively).

In terms of longitudinal grade (i.e., vertical alignment) of roadways, slopes of  $\pm 3\%$ ,  $\pm 6\%$ ,  $\pm 8\%$  and  $\pm 11\%$  were studied in this work, where +i% represents upward grades and -i% represents downward ones. The 0% was also considered, representing a flat gradient (no elevation). These values were assigned based on the maximum longitudinal grade limits for urban Brazilian roadways (DNIT, 2010).

## 4. RESULTS

The built model was firstly adapted (for comparison purposes) with the work of Saad, Mitri and Poorooshasb (2005), where the deflections over time, on the pavement surface (i.e., XY plane in Figure 2) for the case of a flat surface (i = 0%), in a 50 km/h speed were presented. The deflections were measured transversely to the section of the pavement, i.e., along the Y axis – following the 3D coordinate system adopted in this work. They used an implicit FE routine, where the wheel was considered as a load pulse system in order to evaluate the fatigue effects. Thus, after modelling the pavement with its corresponding properties (as similar as possible, considering the intrinsic differences between both models), in Figure 3 the results are presented.

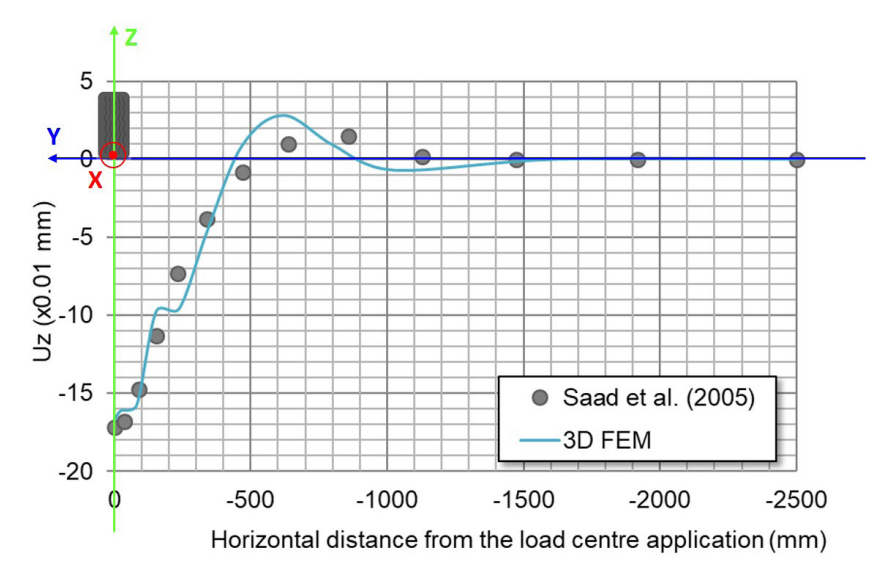


**Figure 3.** The deflections along the (0, -Y, 0) coordinates, obtained in the work of Saad, Mitri and Poorooshasb (2005) and the 3D FEM of this work, for comparison purposes.

As can be observed from Figure 3, this preliminary model presented a very good correspondence with the reference (less than 4% in the worst case) and then it can be considered consistent for the purposes of this research.

Once the model was validated, it was then adapted (regarding to the parameters, load, materials and geometries of this study), and this allowed to obtain 174 combinations cases in a wide cross-analysis study. In the following section only the most significant results are presented, but the reader is invited to consult Figur (2019) work for more details and results.

# 4.1. Speed and acceleration influence

Figure 4a shows the behaviour of the longitudinal stresses ( $S_X$ ) on the X axis along the time, during the wheel movement under constant 40 km/h speed on a flat surface (i = 0%) and intermediate rough surface (FS = 0.68). Also, the deflection basins of the vehicle at 40 km/h, intermediate roughness at three different slope gradients are presented (Figure 4b up to d). The deflections and stresses in this section were read at instant t = 0.178s for a point located at (-1980, 0, 0) coordinates (units in mm), where negative values indicate displacement in the opposite direction of the Z axis. Both (selected time and position) were chosen in order to avoid boundary interference. These results were obtained considering the flat surface (i = 0%), in Figure 4b) and the most severe longitudinal slopes, i.e.,  $i = \pm 11\%$  (in Figure 4c and d). The mentioned sources in caption of Figure 4 have interactive hyperlinks that allow readers to view the generated results (in video format).

According to Figure 4a, there is a succession of tensile (positive values) and compressive (negative values) stresses, at the top and the bottom of the surface layer. The stresses reversed over time, practically reaching the same peak level, in modulus (about 0.30 MPa), inducing the vicinity of the turning point to significant shear stresses. Figure 4a also shows that there is no relevant difference between the absolute values at the top and bottom of the AC layer. This is probably due to the low thickness of the asphalt layer, combined with the fact that it is a (no longer new) material in use. The general results in these graphs showed some numerical fluctuation due to the oscillation in the mesh response and its computational limitation. However, this did not affect the observation of trends in the behaviour nor the amplitude of the responses, as can be seen in these and other results.

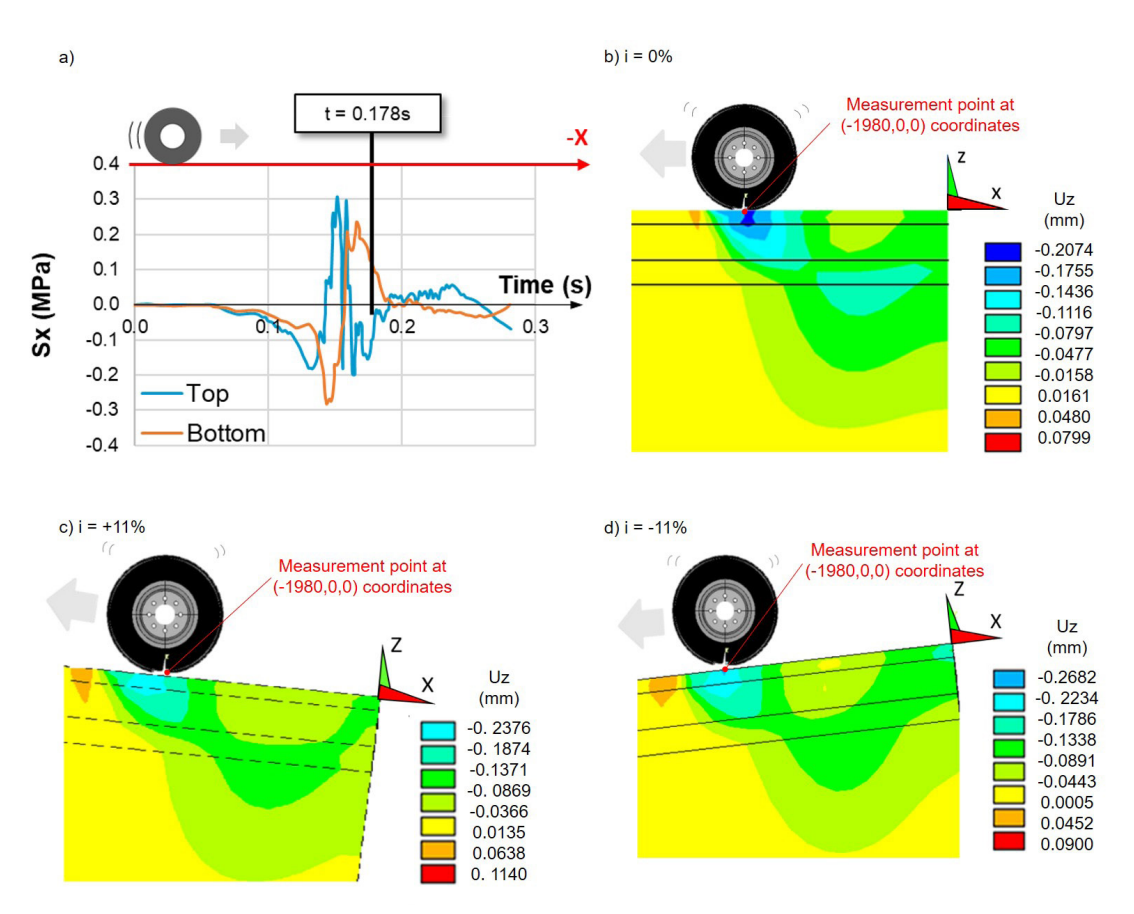


Figure 4. Pavement behaviour at constant speed of 40 km/h: (a) Sx stress components at the top and bottom of the surface layer, for (i=0%) (flat surface) and intermediate roughness ( $F_S=68$ ). Also the deflection  $U_Z$  (mm) for intermediate surface condition is presented, considering: (b) a flat surface (i=0%) (Youtube, 2025a); (c) upward slope (i=+11%) (Youtube, 2025b), and (d) downward slope (i=-11%) (Youtube, 2025c).

Also, from Figure 4b up to d, it can be observed that the deflection basin in the dynamic model is not symmetrical regarding to the load application axis, as considered in pavement analysis or design, presenting a slight inclination to the opposite side of the tyre movement. This indicates the presence of residual displacement (over time) in the pavement immediately after the passage of the tyre, also affecting the layers below the pavement, i.e., the pavement "perceives" the wheel some instants close to its passage.

During the motion, deflections are practically zero in the region in front of the wheel, at the forward movement direction, except for the upper layers, where a slight uplift tendency for material can be observed (i.e., the orange colour indicates positive displacement in the front part close to the wheel, which agrees with the field observation of corrugations). Both (up and down) slopes present slightly more pronounced deflection values than the flat case.

The incidence of Sx (longitudinal) or Sxy (tangential) stresses, and consequently the occurrence of defects, can be further increased in situations of variable slope when there is acceleration and braking of vehicles. This effect was also investigated and it is presented below.

Roughness could have an important role in acceleration/deceleration phenomena. The graph in Figure 5 shows the normalized (i.e., dynamic/static ratio response)  $S_X$  and  $S_{XY}$  stress components on the top layer in a flat pavement, under variable speed, varying the roughness condition and considering two selected extreme velocities (20 and 60 km/h):

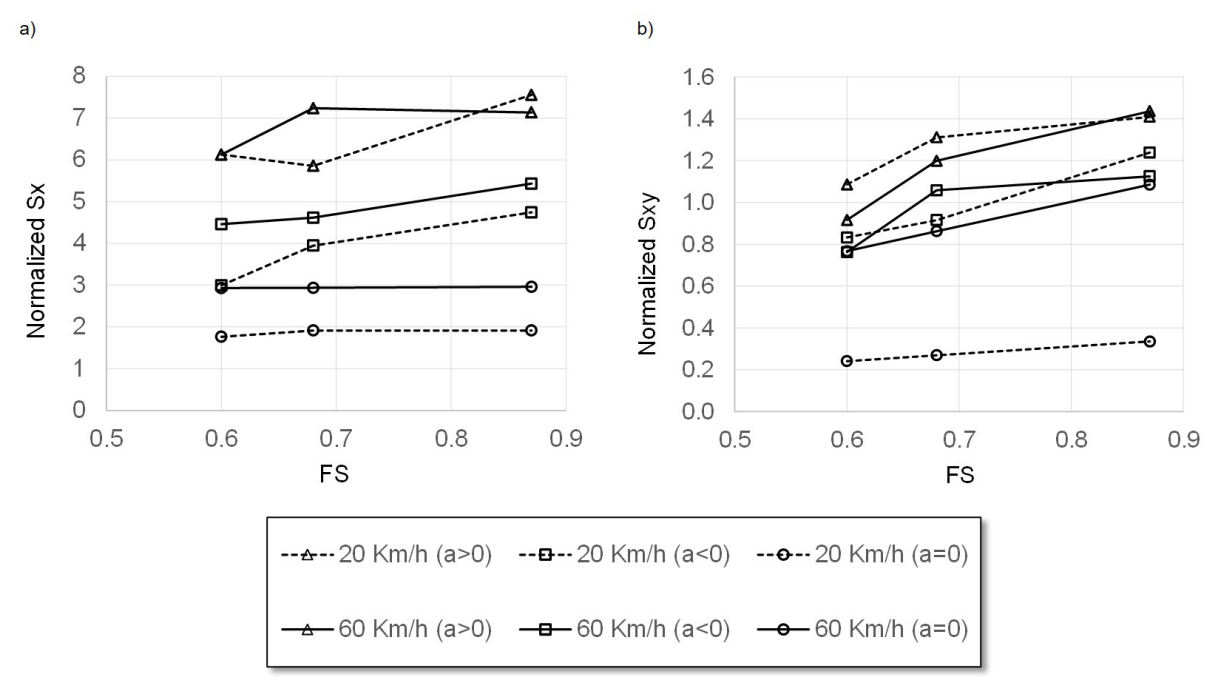


**Figure 5.** Normalized stress components at the top of the coating: (a)  $S_{xy}$ , during acceleration and braking, for (i = 0%), considering roughness.

where a>0 means acceleration, a<0 means deceleration and a=0 means constant speed. The roughness was considered through the FS parameter, where higher the FS, rougher the pavement. It is possible to observe, from Figure 5a, that the highest stresses appear during tyre acceleration, with the dynamic response reaching values around 6 to 7.5 times higher than the static case for Sx (longitudinal stresses). This probably occurs because during acceleration the active forces are higher (in order to overcome inertia effects and quickly move the vehicle), and those forces are also transferred to the pavement. Dynamic tangential stresses (Figure 5b) achieve 1.4 times the static response, in the most severe case. Apparently, shear stresses are more affected by the roughness, where greater the FS (or the roughness), greater the dynamic/static Sxy response under acceleration or deceleration.

The effect of the longitudinal grade on the normalized Sx with variable velocity is also studied, and it is presented in Figure 6.

It can be observed, from Figure 6, that acceleration affects the pavement more than the constant speed condition or even deceleration, in an exponential trend. This is because inertia, associated with the motion effort during the increase or reduction of speed, can amplify the dynamic Sx component (up to 24 times regarding the static response, in the worst case, for i = -11%, from Figure 6b).

Comparing both graphs from Figure 6, when acceleration is considered, downward slopes are more severe than upward ones. And it also can be inferred from the graphs, that greater the speed, higher the  $S_X$  stresses on pavement, when the same acceleration condition is kept (except by the numerical fluctuation between i = +6% and i = +7%).

The behaviour observed in Figures 5 and 6 can be better explained after understanding the main forces involved in the movement, for the main situations considered in this work (Figure 7).

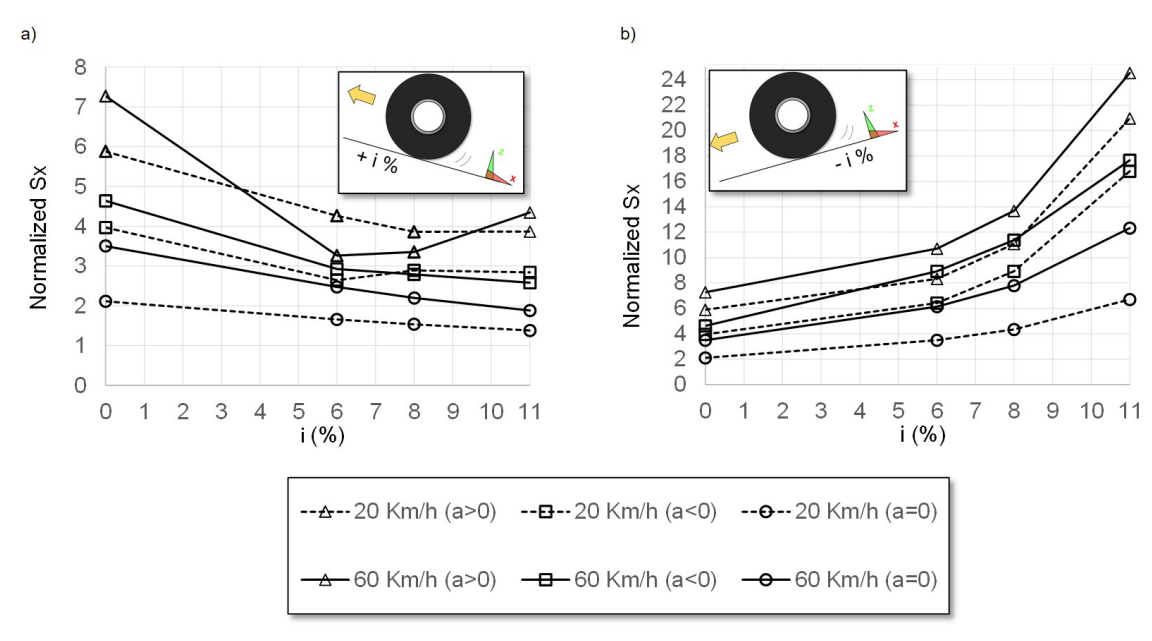


**Figure 6.** Normalized Sx stress component at the top of the AC layer, considering: (a) upslope grade; (b) downslope grade, for variable velocity, grades and intermediate roughness condition.

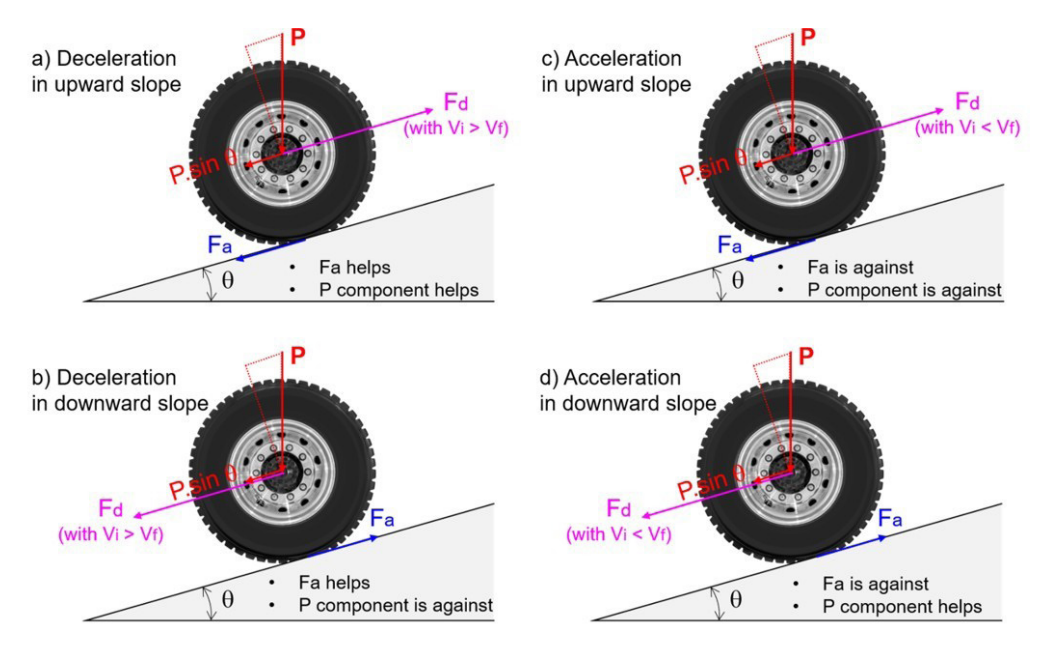


Figure 7. The representation of a wheel in movement on longitudinal slopes: (a) Deceleration ( a < 0 ) in upward slope ( +i% ); (b) Deceleration ( a < 0 ) in downward slope ( -i% ); (c) Acceleration ( a > 0 ) in upward slope ( +i% ); (d) Acceleration ( a > 0 ) in downward slope ( -i% ).

When a wheel is in movement, the main external forces involved are Fd (the displacement force, in the direction of motion, which is supplied by the vehicle's engine and/or the brakes, depending on the situation), Fa (the frictional force, i.e., a force which arises in opposition to the movement between the wheel and the pavement surface) and P (the wheel load, a vertical force dependent on mass), with Fa and P also dependent on gravity. In the situation of Figure 7a), where the vehicle is on an ascending ramp and decelerating, speed is decreasing until it totally stops (where Vi is the

considered initial speed, and Vf is the final speed, which is, in this particular case, equal to zero). In such a situation, the longitudinal component of P (i.e.,  $P \cdot \sin \theta$ ) and the friction Fa are helping to stop the vehicle, so that less efforts are transferred to the pavement and, therefore, less stresses are generated in the pavement surface in response.

Thus, since Fa is the reactive force which will directly activate the stress components in the plane in contact with the wheel (X and Y, according to the adopted coordinate system), it is evident, from Figure 7a up to d that Fa plays an important role in the development of these stresses. Thus, the case of acceleration on a downward slope (Figure 7d) is the one that most affects the Sx stresses (because in this particular case, Fa is the only force that opposes the accelerated movement).

## 5. SUMMARY AND DISCUSSION

In this work, a rolling bus tyre of a standard vehicle in urban flexible pavements was tested in a dynamic 3D FE explicit model. This study aimed to identify critical situations, considering several combinations of some proposed parameters, among which: roughness, roadway longitudinal slope, and speed variation during vehicle acceleration and braking.

The main considerations in terms of the parameters inserted into the proposed model allow to establish that the slope have an important influence on the longitudinal stress ( $S_X$ , along the X axis, i.e., the tyre displacement direction) and shear stress ( $S_X$ , parallel to the surface's plane), mainly at the top of the coating layer. The stress components which were chosen for this study are generally associated to the failure initiation in pavements (as  $S_X$  tensile stress is related to the crack opening and  $S_{XY}$  shear stress is related to corrugations). Actually, the design methods currently used in Brazil for flexible pavements do not consider shear stresses, resulting in structures with lesser resistance to this type of effort, which is probably related to the defects that commonly arise in inclined planes and heavy bus stops or corridors.

Under constant speed, it is observed that normalized Sx and Sxy stresses present small variation with the increasing roughness on the top of the AC layer. On the other hand, it can be significant for shear stresses Sxy (where an increase of approximately 40% under acceleration is observed) or for longitudinal stresses, where the dynamic Sx is up to 7 times greater than the static Sx, in acceleration condition.

According to this work, upward slopes generally tend to reduce Sx stresses, while steeper downward slopes tend to increase them. When vehicle speed variation is considered, acceleration is slightly more severe than deceleration, and downward slope is more severe than upslope grades, presenting exponential variation with the grades. This occurs because when moving downhill, the resultants of the dynamic forces add to the gravitational forces, and during acceleration, more efforts are transferred to the pavement to start moving the vehicle, taking it out of its resting state. Therefore, at the beginning of the acceleration process, its status is closest to the static one, which is more conservative. The most critical situation for the top AC layer, in terms of longitudinal stresses, was found during tyre acceleration, where dynamics can amplify about 7.5 times the static response for flat surfaces i = 0%, but can reach up to 24 times for higher downslope grades.

For the purposes of this work, the dynamic effects could be neglected at the top of the subgrade (less than 0.10mm). The bottom of the AC layer exhibits a similar response to the surface; thus, it was also neglected in the next studies.

In motion, the shape of the deflectometric basin is visibly affected by acceleration and longitudinal grade, showing a slight asymmetry, contrasting with the shape of the traditional static model.

The shape tends to be more elongated to the opposite side to the tyre displacement, indicating the action of residual deflection in the pavement immediately after the passage of the vehicle. From this observation, it is important to notice that, when the pavement's basin is obtained in an inclined plane, overshadowed results can be obtained from the model commonly employed by the standards, which mathematically considers a symmetric basin in a flat surface.

The findings of this work are compatible with the type of defects observed on flexible pavements in the studied bus corridors in Curitiba, whose problems appear mostly at the surface of the AC layer. As a preventive measure, the city hall has gradually replaced flexible pavement in bus stop areas with concrete slabs.

#### **AUTHORS' CONTRIBUTIONS**

NEF: Conceptualization, Validation, Data curation, Investigation, Writing – original draft and Writing – review & editing; DFV: Formal analysis, Resources, Investigation, Supervision, Writing – review & editing.

## **CONFLICTS OF INTEREST STATEMENT**

The authors have no conflicts of interest to declare.

## **USE OF ARTIFICIAL INTELLIGENCE-ASSISTED TECHNOLOGY**

Only support or verification tools were used to translate specific excerpts or terms (e.g., Google Translate) or AI photo enhancer for images. This work was carried out by using human intelligence and traditional research methods.

## **DATA AVAILABILITY STATEMENT**

The data which support the results of this study are not openly available because the authors intend to continue this research, using internally the archives in the future, and thus deepen even more the understanding of pavement failure mechanisms.

#### **ACKNOWLEDGEMENTS**

The authors would like to thank CAPES for the financial support granted to the first author of this paper. This work was carried out in the Group of Advanced Research and Development of Infrastructures and the Graduate Program in Civil Engineering at the Federal University of Paraná.

## **REFERENCES**

Assogba, O.C.; Y. Tan; Z. Sun *et al.* (2021) Effect of vehicle speed and overload on dynamic response of semi-rigid base asphalt pavement. *Road Materials and Pavement Design*, v. 22, n. 3, p. 572-602. DOI: 10.1080/14680629.2019.1614970.

ASTM (2023) ASTM E 1960-98: Standard Practice for Calculating International Friction Index of a Pavement Surface. West Conshohocken, PA: ASTM

Brasil (1997) Lei nº 9.503. Institui o Código de Trânsito Brasileiro. *Diário Oficial da República Federativa do Brasil*. Brasília. Available at: <a href="https://www.planalto.gov.br/ccivil\_03/leis/19503.htm">https://www.planalto.gov.br/ccivil\_03/leis/19503.htm</a> (accessed 03/27/2025).

Chen, B.; X.C. Wang and K. Mu (2011) Mechanical response of longitudinal slope segments based on Burgers Model. *Advanced Materials Research*, v. 243, n. 249, p. 4172-4177. DOI: 10.4028/www.scientific.net/AMR.243-249.4172.

CNT (2018) Conheça os 13 Principais Defeitos do Pavimento das Rodovias. Available at: <a href="http://www.cnt.org.br/imprensa/noticia/conheca-principais-defeitos-pavimento">http://www.cnt.org.br/imprensa/noticia/conheca-principais-defeitos-pavimento</a> (accessed 03/27/2025).

DNIT (2006) Manual de Restauração de Pavimentos Asfálticos (3a ed., No. IPR-720). Rio de Janeiro: DNIT.

DNIT (2010) Manual de Projeto Geométrico de Travessias Urbanas (No. IPR-740). Rio de Janeiro: DNIT.

DNIT (2012) *Quadro de Fabricantes de Veículos*. Rio de Janeiro: DNIT. Available at: <a href="https://www.gov.br/dnit/pt-br/rodovias/operacoes-rodoviarias/pesagem/QFV2012ABRIL.pdf">https://www.gov.br/dnit/pt-br/rodovias/operacoes-rodoviarias/pesagem/QFV2012ABRIL.pdf</a> (accessed 03/27/2025).

DNIT (2013) Norma DNIT 005/2003-TER. Defeitos nos Pavimentos Flexíveis e Semi-Rígidos Terminologia. Rio de Janeiro: DNIT.

Farias, M.M. (1997) The influence of horizontal loads on the fatigue of pavements'. *In Symposium on Recent Developments in Soil and Pavement Mechanics*. Rio de Janeiro, pp. 359-365. Available at: <a href="http://worldcat.org/isbn/9054108851">http://worldcat.org/isbn/9054108851</a>> (accessed 03/27/2025).

- Feng, L.; J. Liu; H. Wang *et al.* (2012) Shear stress of asphalt pavement in steep slope sections. *In International Conference on Transportation Engineering 2009*. ASCE, p. 869-874. DOI: 10.1061/41039(345)144.
- Figur, N.E. (2019) Estudo das Tensões e Deflexões em Pavimentos Flexíveis Devido à Atuação de Cargas Dinâmicas dos Veículos: Uma Análise Numérica. Dissertação (mestrado). Universidade Federal do Paraná. Curitiba. Available at: <a href="https://hdl.handle.net/1884/63115">https://hdl.handle.net/1884/63115</a> (accessed 03/27/2025).
- Ghoreishy, M.H.R. (2006) 'Finite element analysis of the steel-belted radial tyre with tread pattern under contact load'. *Iranian Polymer Journal*, v. 15, n. 8, p. 667-674.
- Giurgiu, T.; F. Ciortan and C. Pupaza (2013) Static and transiente analysis of radial tires using ANSYS. *In Recent Advances in Industrial and Manufacturing Technologies: Proceedings of the 1st International Conference on Industrial and Manufacturing Technologies (INMAT'13)*. Athens, p. 148-152. Available at: <a href="https://www.researchgate.net/publication/301560795\_Static\_and\_Transient\_Analysis\_of\_Radial\_Tires\_Using\_ANSYS">https://www.researchgate.net/publication/301560795\_Static\_and\_Transient\_Analysis\_of\_Radial\_Tires\_Using\_ANSYS> (accessed 03/27/2025).
- Hajj, E.Y.; P. Thushanthan; P.E. Sebaaly *et al.* (2012) Influence of tyre-pavement stress distribution, shape, and braking on performance predictions for asphalt pavement. *Transportation Research Record: Journal of the Transportation Research Board*, v. 2306, n. 1, p. 73-85. DOI: 10.3141/2306-09.
- Hammoum, F.; A. Chabot; D. St-Laurent *et al.* (2010) Effects of accelerating and decelerating tramway loads on bituminous pavement. *Materials and Structures*, v. 43, n. 9, p. 1257-1269. DOI: 10.1617/s11527-009-9577-9.
- Khavassefat, P.; D. Jelagin and B. Birgisson (2014) Dynamic response of flexible pavements at vehicle–road interaction. *Road Materials and Pavement Design*, v. 16, n. 2, p. 256-276. DOI: 10.1080/14680629.2014.990402.
- Kuo, C.M.; K.T. Hall and M.I. Darter (1995) Three-dimensional finite element model for analysis of concrete pavement support. *Transportation Research Record: Journal of the Transportation Research Board*, n. 1505, p. 119-127.
- Li, C. and L. Li (2012) Criteria for controlling rutting of asphalt concrete materials in sloped pavement. *Construction & Building Materials*, v. 35, p. 330-339. DOI: 10.1016/j.conbuildmat.2012.04.003.
- Li, Y.C. and Y.Y. Xin (2014) The dynamic response of large longitudinal slope of asphalt road pavement under heavy impulsive load. *Advanced Materials Research*, v. 1065-1069, p. 806-813. DOI: 10.4028/www.scientific.net/AMR.1065-1069.806.
- Medina, J. and L.M.G. Motta (2015) Mecânica dos Pavimentos (3a ed.). Rio de Janeiro: Interciência.
- Meyers, M.A. and K.K. Chawla (2009) Mechanical Behaviour of Materials (2nd ed.). Cambridge: Cambridge University Press.
- Nonde, L. (2014) Effect of vertical and horizontal load on pavement interface shear stress. *International Journal of Engineering Research & Technology*, v. 3, n. 10, p. 1295-1299.
- Saad, B.; H. Mitri and H. Poorooshasb (2005) Three-dimensional dynamic analysis of flexible conventional pavement foundation. *Journal of Transportation Engineering*, v. 131, n. 6, p. 460-469. DOI: 10.1061/(ASCE)0733-947X(2005)131:6(460).
- Saleh, M.F.; M.S. Mamlouk and E.B. Owusu-Antwi (2000) Mechanistic roughness model based on vehicle-pavement interaction. Transportation Research Record: Journal of the Transportation Research Board, v. 1699, n. 1, p. 114-120. DOI: 10.3141/1699-16.
- Schmidt, E.P. and C.E.N.A. Mazzilli (2017) Influência da flexibilidade do tabuleiro na resposta dinâmica de pontes rodoviárias curvas. *Revista IBRACON de Estruturas e Materiais*, v. 10, n. 3, p. 706-743. DOI: 10.1590/s1983-41952017000300009.
- Seco, R. (2016) *Curitiba, 'Cidade Modelo', Busca Novas Referências: 'Ao Menos Não Somos São Paulo'*. Available at: <a href="http://brasil.elpais.com/brasil/2016/06/30/politica/1467311191\_496018.html">http://brasil.elpais.com/brasil/2016/06/30/politica/1467311191\_496018.html</a> (accessed 03/27/2025)
- URBS (2017a) Composição da Frota. Curitiba. Available at: <a href="https://www.urbs.curitiba.pr.gov.br/transporte/rede-integrada-de-transporte/42">https://www.urbs.curitiba.pr.gov.br/transporte/rede-integrada-de-transporte/42</a> (accessed 03/27/2025).
- URBS (2017b) *Características da RIT*. Curitiba. Available at: <a href="https://www.urbs.curitiba.pr.gov.br/transporte/rede-integrada-de-transporte/18">https://www.urbs.curitiba.pr.gov.br/transporte/rede-integrada-de-transporte/18</a>> (accessed 03/27/2025).
- Yang, J.; W. Li; Z. Yu et al. (2010) Finite element analysis of asphalt pavement on long-steep longitudinal slope. *Journal of Traffic and Transportation Engineering*, v. 10, n. 6, p. 20-24. DOI: 10.19818/j.cnki.1671-1637.2010.06.004.
- Yin, Y.; H. Wen; L. Sun *et al.* (2020) The influence of road geometry on vehicle rollover and skidding. *International Journal of Environmental Research and Public Health*, v. 17, n. 5, p. 1648. DOI: 10.3390/ijerph17051648. PMid:32138346.
- Youtube (2025a) *Pavement Deflections, for i=0% 40Km/h (at Constant Speed, Intermediate Rough Surface*). Available at: <a href="https://youtu.be/p0ejW8zLGLo">https://youtu.be/p0ejW8zLGLo</a> (accessed 03/27/2025).
- Youtube (2025b) Pavement Deflections, for i=+%11 40Km/h (at Constant Speed, Intermediate Rough Surface). Available at:  $\frac{1}{2000}$  <a href="https://youtu.be/RHZu1SSu90Y">https://youtu.be/RHZu1SSu90Y</a> (accessed 03/27/2025).
- Youtube (2025c) Pavement Deflections, for i=-11% 40Km/h (at Constant Speed, Intermediate Rough Surface). Available at: <a href="https://youtu.be/37UFyhxDUhg">https://youtu.be/37UFyhxDUhg</a> (accessed 03/27/2025).
- Zaghloul, S. and T. White (1993) Use of a three-dimensional, dynamic finite element program for analysis of flexible pavement. *Transportation Research Record: Journal of the Transportation Research Board*, n. 1388, p. 60-69.
- Zhang, N.M. and X.D. Wang (2010) Deformation analysis of pavement structures under coexistence of vertical and horizontal loads. *Applied Mechanics and Materials*, v. 44-47, p. 3053-3059. DOI: 10.4028/www.scientific.net/AMM.44-47.3053.
- Zhang, H.; M. Yang and Y. Ma (2020) Study on the performance of high-modulus asphalt concrete pavement in extreme curves or steep slopes of trunk highway. *Stavební Obzor Civil Engineering Journal*, v. 29, n. 1, p. 97-109. DOI: 10.14311/CEJ.2020.01.0009.